J Neuropathol Exp Neurol
Vol. 71, No. 5
May 2012
pp. 398Y412

ORIGINAL ARTICLE

Acute Rejection of Myofibers in Nonhuman Primates: Key Histopathologic Features

Daniel Skuk, MD

Abstract

The aim of this study was to define the histologic features of acute rejection of myofibers, particularly in the context of therapeutic myogenic cell transplantation. Myoblasts expressing or not expressing A-galactosidase were transplanted into 13 macaques that were divided into 3 protocols: withdrawal of immunosuppression, low immunosuppression, and progressive reduction of immunosuppression. The biopsy samples were obtained from cell-grafted sites at different intervals, and cryostat sections of biopsies were analyzed. The grafts were lost in all the monkeys at different periods after transplantation depending on the protocol and in association with low blood levels of tacrolimus. In all cases, graft loss was associated with the presence of dense focal accumulations of CD8-positive and CD4-positive lymphocytes and a component of macrophages. The lymphocyte accumulations totally or partially surrounded some myofibers and often invaded them; they were mainly endomysial. These histopathologic patterns in nonhuman primates and their similarity with preliminary observations in humans may facilitate the translation of these results to the histologic diagnosis of acute rejection of myofibers in human clinical trials of myogenic cell transplantation and probably gene therapy.

Key Words: Acute rejection, Cell transplantation, Histopathology, Myofiber, Skeletal muscle.

INTRODUCTION

Myogenic cell transplantation has potential application for the treatment of myopathies (1). Excluding purely autologous cell transplantation, graft survival depends on the control of acute rejection. The control of acute rejection is limited in clinical practice because of toxicities of immunosuppression, and monitoring is essential to treat acute rejection and to preserve the graft. Histopathologic analysis is currently the only reliable method for monitoring and diagnosing acute rejection in clinical organ transplantation (2Y4). In the context of myogenic cell transplantation, however, there are no histologic criteria to diagnose acute rejection. For example, our laboratory conducted clinical trials in which myoblasts from nonmyopathic donors were transplanted in patients with Duchenne muscular dystrophy (5, 6). We used tacrolimus for immunosuppression, as we do for myoblast allotransplantation in mice (7, 8) and monkeys (9, 10). Beyond the demonstration that a better protocol for cell injection allowed better results than in previous clinical trials (1), acute rejection was difficult to diagnose in this context. Histologic analysis showed immune cells (CD8-positive and CD4-positive cells and macrophages), both in myoblast-grafted sites and in control (nongrafted) sites in all patients (5). The presence of immune cells in control sites was explained by the fact that skeletal muscles in Duchenne muscular dystrophy exhibit chronic infiltrates of immune cells (11, 12). Therefore, it was important to compare cell-grafted sites with control sites to analyze the immune response to the grafts. In most patients, one or more immune cells were more abundant in the cell-grafted site than in the control site. The question that remained open was to what extent this could be an expression of ongoing acute rejection.

A literature review reveals a lack of histopathologic studies on the acute rejection of allogeneic myofibers. Previous clinical trials of myoblast transplantation in patients with myopathy were not helpful because most grafts were unsuccessful, mainly because of poor technique of transplantation (1), and therefore, it was not possible to analyze immune responses against the graft. The only available studies illustrating the histology of the immune response after transplantation of myogenic cells have been carried out in mice (13Y18). In large part, those studies were carried out to determine whether the transplanted myoblasts triggered an immune response, and most of them examined the rapid rejection of these mononuclear cells in immunocompetent animals rather than late rejection of allogeneic myofibers. In the few cases in which rejection of myofibers was observed, the histologic observations were succinct and not the primary aim of the study (15, 17). Moreover, the immunologic differences between mice and humans (19) make direct extrapolation of mouse experiments to clinical transplantation difficult.

We have been using nonhuman primates of the genus Macaca to analyze the transplantation of myogenic cells in a model more relevant to humans. The close phylogenetic relationship between humans and macaques (both are primates of the parvorder Catarrhini) provides optimal antigenic and immunologic similarities to preclinical transplantation

From the Neurosciences Division, Human Genetics, CHUQ Research Center, Centre Hospitalier de l'Université Laval, Quebec, Canada.
Send correspondence and reprint requests to: Daniel Skuk, MD, Unité de recherche en Génétique humaine, Centre Hospitalier de l'Université Laval, 2705 Blvd Laurier, Quebec, Canada G1V 4G2; E-mail: Daniel.Skuk@fmed.ulaval.ca
This work was supported by grants of the Jesse's Journey Foundation for Gene and Cell Therapy of Canada and the Association Fran0aise contre les Myopathies to Dr Daniel Skuk.

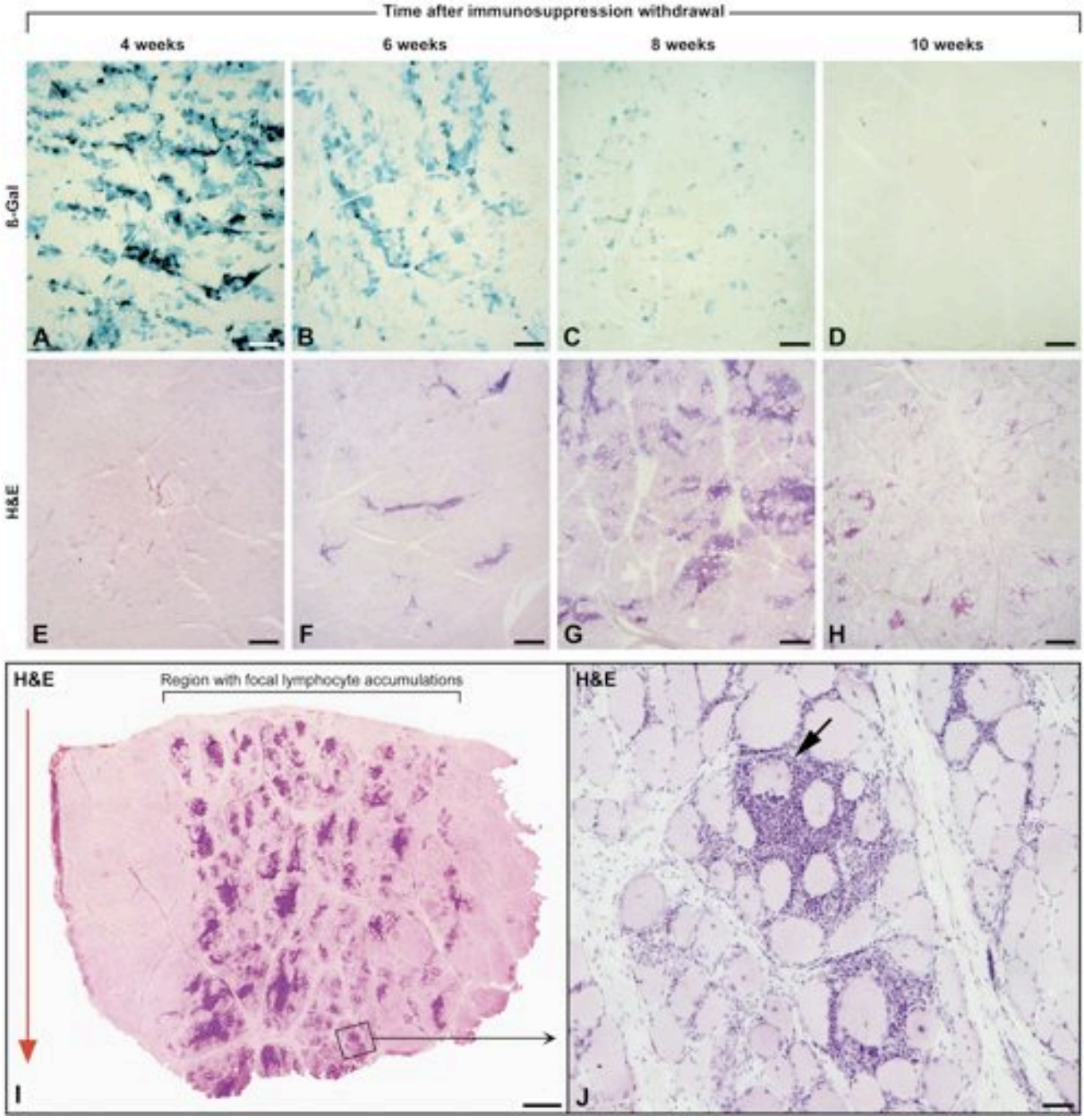

FIGURE 1. Graft rejection in the immunosuppression withdrawal (IW) group. (AYH) Cross sections of muscle biopsies performed at sites grafted with A-galactosidase (A-Gal)Ylabeled myoblasts in monkey IW-2. A to D (A-Gal detection) and E to H (corresponding hematoxylin and eosinYstained serial sections) illustrate respectively the evolution of the graft and the muscle histology. Many A-GalYpositive myofibers are observed at 4 and 6 weeks after tacrolimus withdrawal (A, B). The structure of muscle tissue is normal at Week 4 (E). Focal lymphocyte accumulations appear at Week 6 (F). The amount of A-GalYpositive myofibers decreased noticeably in Week 8 (C) concomitant with focal lymphocyte accumulations (G). No A-GalYpositive myofibers are observed at Week 10 (D) and some focal lymphocyte accumulations remain (H). (I, J) Complete cross section of the biopsy performed at the peak of infiltration in the monkey IW-1 (8 weeks after tacrolimus withdrawal). There are focal dense lymphocyte infiltrates. The epimysium is at the top and the red arrow indicates the original trajectory of the cell injections. The square in I is shown at higher magnification in J. The lymphocyte accumulations are in the endomysium, completely or partially surrounding some myofibers and invading some of them (J, arrow). Scale bars = (AYH) 0.5 mm (magnification is the same for these images); (I) 1 mm; (J) 50 Km.

research (20Y22). Unlike mice, macaques share with humans important transplantation immune parameters, including conserved homology in the genes that encode the major histocompatibility complex (MHC) and the T-cell receptor (23Y26). Importantly for the present study, the rejection of allografts in nonhuman primates is driven by the same immune elements as in humans, showing comparable histologic features and temporal evolution (22). For example, nonhuman primates have been used to define the histopathology of acute rejection in limb transplantation rather than using results obtained in rats, rabbits, dogs, or pigs, some of which were not transferable to humans (27). For these reasons, nonhuman primates are considered to be a crucial model for clinical extrapolation in transplantation research (20Y22).

The present study was conducted in macaques to define the main histologic features of acute rejection of allogeneic myofibers with potential application to the clinic.

MATERIALS AND METHODS

Animals

Cynomolgus monkeys (Macaca fascicularis, n = 13, males and females; age range, 44Y57 months) received transplantation of allogeneic myoblasts. For transplantation and biopsies, they were kept under general anesthesia using isoflurane (1.5%Y2% in oxygen) after induction with ketamine (10 mg/kg) and glycopyrrolate (0.05 mg/kg) intramuscularly (i.m.). Buprenorphine (0.01 mg/kg twice a day for 3 days) was

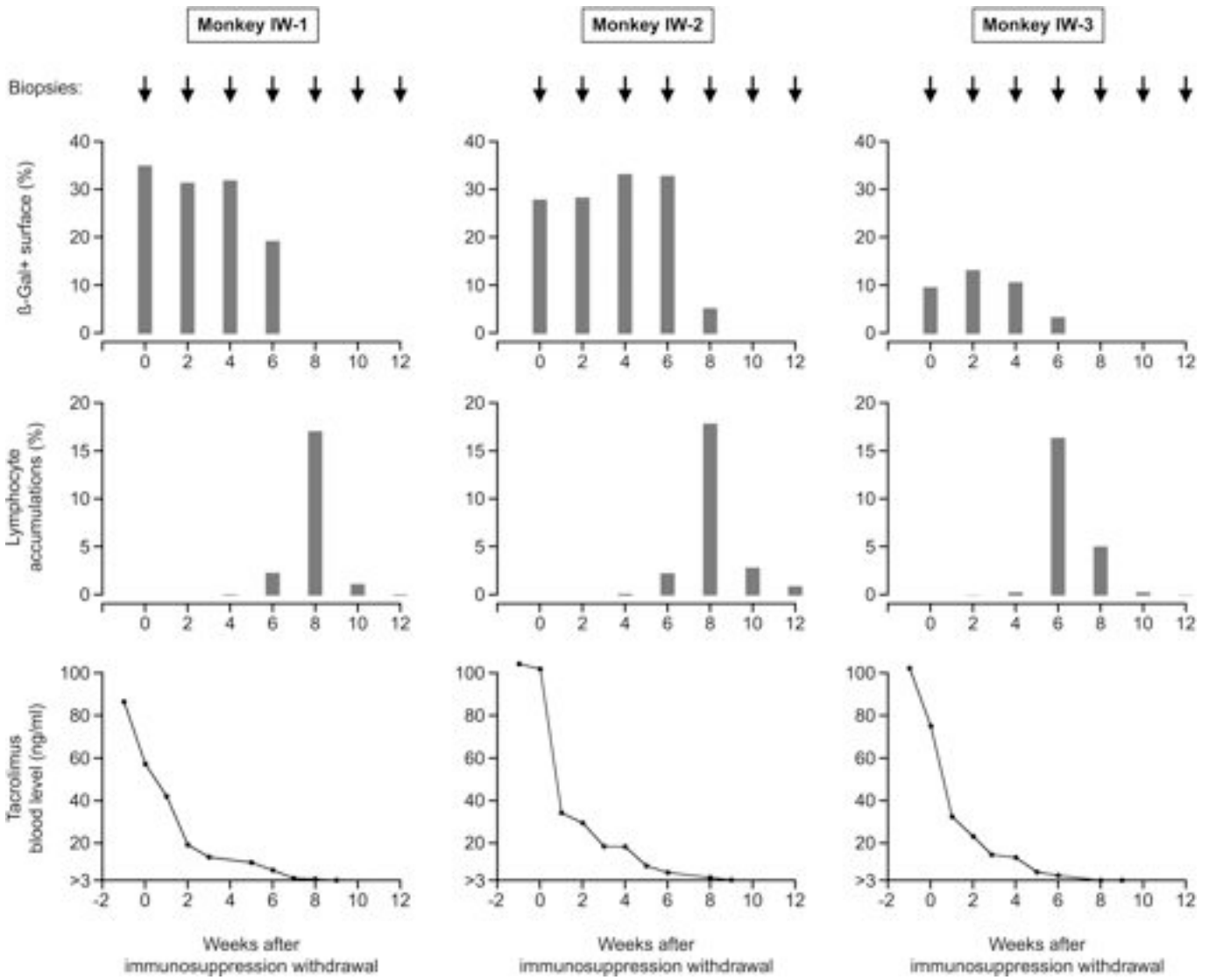

FIGURE 2. Graphical representation of graft evolution and lymphocyte accumulations in the 3 monkeys grafted with A-galactosidase (A-Gal)Ylabeled myoblasts in the immunosuppression withdrawal (IW) group. The chronological correlation between graft loss and lymphocyte infiltration is compared to tacrolimus blood levels. Arrows indicate the biopsy time points. The y axes are at the same scale for each parameter.

given for postoperative analgesia. Because of the many muscle samples done in some animals, they were killed at the end of the experiment by intravenous administration of a pentobarbital overdose (120 mg/kg) after anesthesia using ketamine (15 mg/kg) i.m. The Laval University Animal Care Committee authorized these procedures.

Immunosuppression

An i.m. formulation of tacrolimus (a generous gift from Astellas Pharma, Inc, Osaka, Japan) was administered once a day for immunosuppression, beginning 5 to 7 days before transplantation. Blood samples were taken at different intervals to quantify tacrolimus blood levels using an IMx tacrolimus II

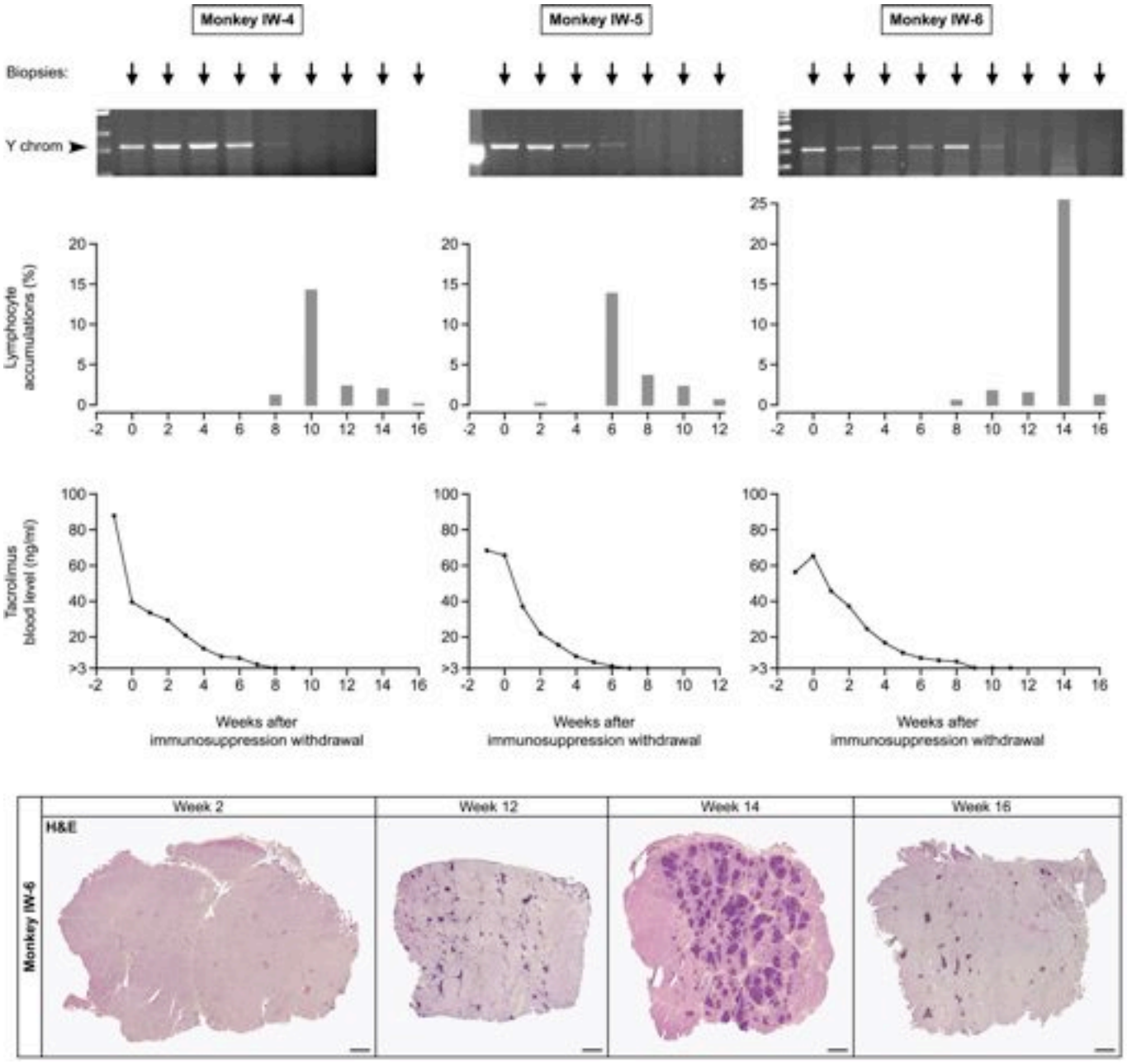

FIGURE 3. Graphical representation of the evolution of the lymphocyte accumulations in the 3 female monkeys in the immunosuppression withdrawal (IW) group grafted with male myoblasts (A-galactosidase [A-Gal] negative). The Y chromosome polymerase chain reaction products detected by electrophoresis are shown in the top. There is a temporal correlation in the progression of graft loss (Y chromosome), the magnitude of lymphocyte infiltration and decreasing tacrolimus blood levels. Arrows in the top indicate the biopsies. The y axes are at the same scale for each parameter. Panels in the bottom show complete cross sections of muscle biopsies performed in the cell-grafted sites in monkey IW-6 and illustrate the lymphocyte infiltrates in hematoxylin and eosin stains at representative time points. Scale bars = 1 mm (magnification is the same for these images).

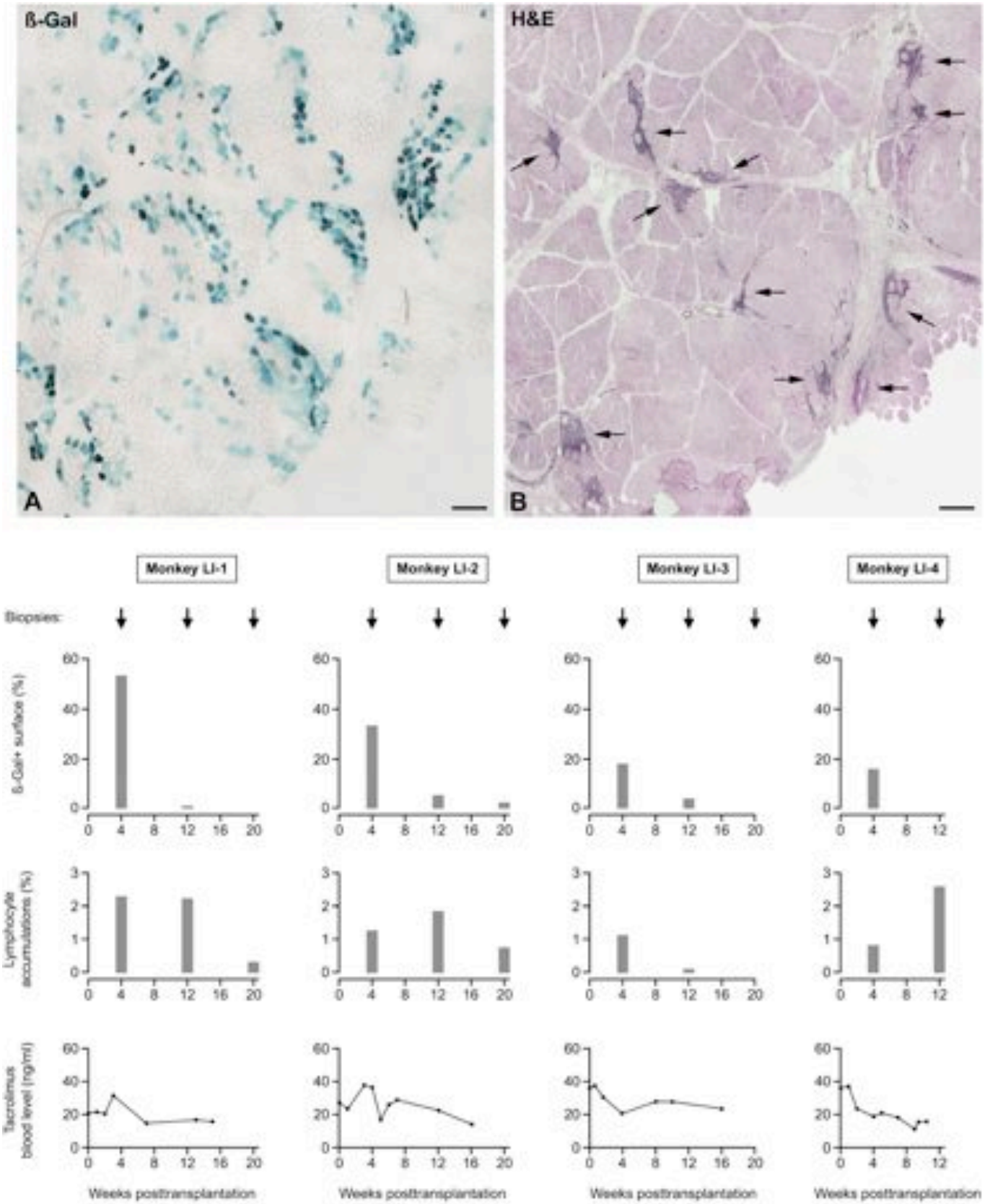

kit for microparticle enzyme immunoassay (Abbott, Wiesbaden, Germany).

Graft Monitoring

To monitor the graft by histology in some monkeys, we labeled the grafted cells with A-galactosidase (A-Gal). To confirm that the immune findings were due to the allogeneic context and not to the expression of A-Gal, we also grafted cells that were not labeled with A-Gal. To monitor graft survival in this case, we grafted male cells in females and detected the Y chromosome with polymerase chain reaction (PCR).

Cell Transplantation

Two cell lines were obtained from skeletal muscle biopsies performed in 2 other cynomolgus monkeys. The biopsies were minced with fine scissors into fragments of less than 1 mm^3 and then dissociated with 0.2% collagenase (Sigma, St. Louis, MO) in Hanks balanced salt solution (HBSS) for 1 hour, followed by another dissociation in 0.125% trypsin (Gibco, Grand Island, NY) in HBSS for 45 minutes. The isolated cells were subcultured in vitro in MCDB-120 culture medium (28) with 15% fetal bovine serum (HyClone, Logan, UT), 10 ng/ml basic fibroblast growth factor (Feldan, St. Laurent, Quebec, Canada), 0.5 mg/ml bovine serum albumin (Sigma), 0.39 Kg/ml dexamethasone (Sigma), and 5 Kg/ml human insulin (Sigma).

One of the cell lines was infected twice in vitro with a replication-defective retroviral vector LNPOZC7 (gift from Dr Constance Cepko, Harvard Medical School, Boston, MA) encoding a LacZ reporter gene and a neomycin resistance gene. The transduced cells were selected twice with 600 Kg/ml Geneticin (Invitrogen, Burlington, Ontario, Canada) within 4 days, proliferated until confluence, and frozen for storage in liquid N_2. The other cell line (from a male donor) was proliferated without any genetic modification.

A sample of cells to be frozen was analyzed to determine the percentage of CD56-positive cells as an indicator of the percentage of myoblasts. These cells were incubated with a phycoerythrin-coupled anti-CD56 antibody (Beckman Coulter, Fullerton, CA) and analyzed by flow cytometry. Respectively, 99% (A-GalYlabeled) and 98% (nonYA-GalYlabeled) cells were CD56-positive. Additional details on the cell culture have been published previously (29).

For transplantation, cells were thawed, proliferated by 1 or 2 passages in culture, detached from the flasks with 0.1% trypsin, and washed 3 times with HBSS. The final cell pellets were resuspended in HBSS and injected as indicated in the next paragraphs. The muscles used for transplantations were the left and right biceps brachii, quadratus femoris, and gastrocnemius.

Cell transplantation was performed percutaneously by parallel equidistant injections placed approximately 1 mm apart, perpendicular to the surface of the muscle, using 27-gauge needles of 0.5 in. Most transplantations were performed with a 250-KL syringe (Hamilton, Reno, NV) attached to a PB600-1 repeating dispenser (Hamilton) (30). Some muscles were grafted using 100-KL syringes (Hamilton) not attached to dispensers (2 monkeys), a multisyringe dispenser (Matrix Technology Corp, Hudson, NH; 1 monkey) (30), or a semimanual device specific for repetitive intramuscular injections (31) (1 monkey). The amount of cells injected per cubic centimeter of muscle (K = 22.7 10^6 T 4.4 10^6 [SD]) varied with the total number of cells produced at the time of transplantation. These amounts exceeded the optimal number of cells (10 $10^6/cm^3$ of muscle) determined in previous studies. Each cell injection consisted of needle penetration to full depth and delivery of 5 to 10 KL of cell suspension during the withdrawal of the needle. An OpSite sterile transparent dressing with a 5-mm grid (Smith & Nephew, Hull, UK) was adhered to the skin to control the pattern of injections. Most transplants were performed on small sites (covering an area of È1 cm^2), but some were made in the whole muscle. To identify the injected muscle sites during biopsies, 2 stitches of inert nonabsorbable polypropylene 4.0 suture (Prolene; Ethicon, Inc, Somerville, NJ) were placed È5 mm on both sides of each site. Up to 3 sites of 1 cm^2 were grafted per biceps brachii and quadratus femoris and up to 2 sites of 1 cm^2 per gastrocnemius. These sites were separated by 0.5 to 1.5 cm. Additional details on cell transplantation protocol have been reported (29).

Immunosuppression Protocols

We used 3 different immunosuppression protocols as follows:

Immunosuppression withdrawal (IW) group. To induce clear rejection of the allogeneic myofibers once the graft was stable (after the fusion of the grafted myoblasts with the myofibers), we immunosuppressed monkeys at optimal levels for 1 month and then stopped the immunosuppression to induce rejection. We targeted tacrolimus blood levels that we knew would ensure the survival of the graft during the first month after myoblast allotransplantation (950 Kg/L).

To observe immune reactions in recipients in which the immunosuppression was insufficient from the beginning to prevent acute rejection, we immunosuppressed monkeys in suboptimal levels for several weeks. In this low-immunosuppression (LI) group, we targeted suboptimal tacrolimus blood levels (30Y20 Kg/L) until the end of the experiment.

To reproduce the situation of an immunosuppressed recipient in whom acute rejection occurs several months after transplantation, we included 3 monkeys in which immunosuppression was maintained at optimal levels for a month and then gradually reduced until graft loss was observed several months later. In this immunosuppression reduction (IR)

FIGURE 4. Low-immunosuppression (LI) group. (A, B) Serial cross sections of a muscle biopsy performed at 1 month after transplantation in a cell-grafted site stained for histochemical detection of A-galactosidase (A-Gal) (A) and with hematoxylin and eosin (B). Many A-GalYpositive myofibers are present (A) along with several focal lymphocyte accumulations close to the A-GalYpositive myofibers (B, arrows indicate most of the focal lymphocyte accumulations). Graphs demonstrate the evolution of the grafts, lymphocyte infiltrates, and tacrolimus blood levels for each monkey. The arrows indicate the biopsy time points. The y axes are at the same scale for each parameter. Scale bars = 250 Km.

group, we targeted high tacrolimus blood levels during the first month after transplantation; tacrolimus levels were then gradually reduced to 40, 20, or 10 Kg/L and even lower.

The number of monkeys used in each experimental group was as follows: IW group, n = 6 (of which 3 received A-GalYlabeled myoblasts and 3 received myoblasts that were not genetically modified and male-derived myoblasts were transplanted in female recipients to monitor the graft survival by PCR detection of the Y chromosome); LI group, n = 4; and IR group, n = 3. Monkeys in the LI and IR groups received A-GalYlabeled myoblasts. Hence, the monkeys are referred to according to the experimental group, for example, monkey IW-1, monkey IW-2, etc.

Sampling

Biopsies were performed in the cell-grafted sites at different periods after transplantation. In the IW group, they

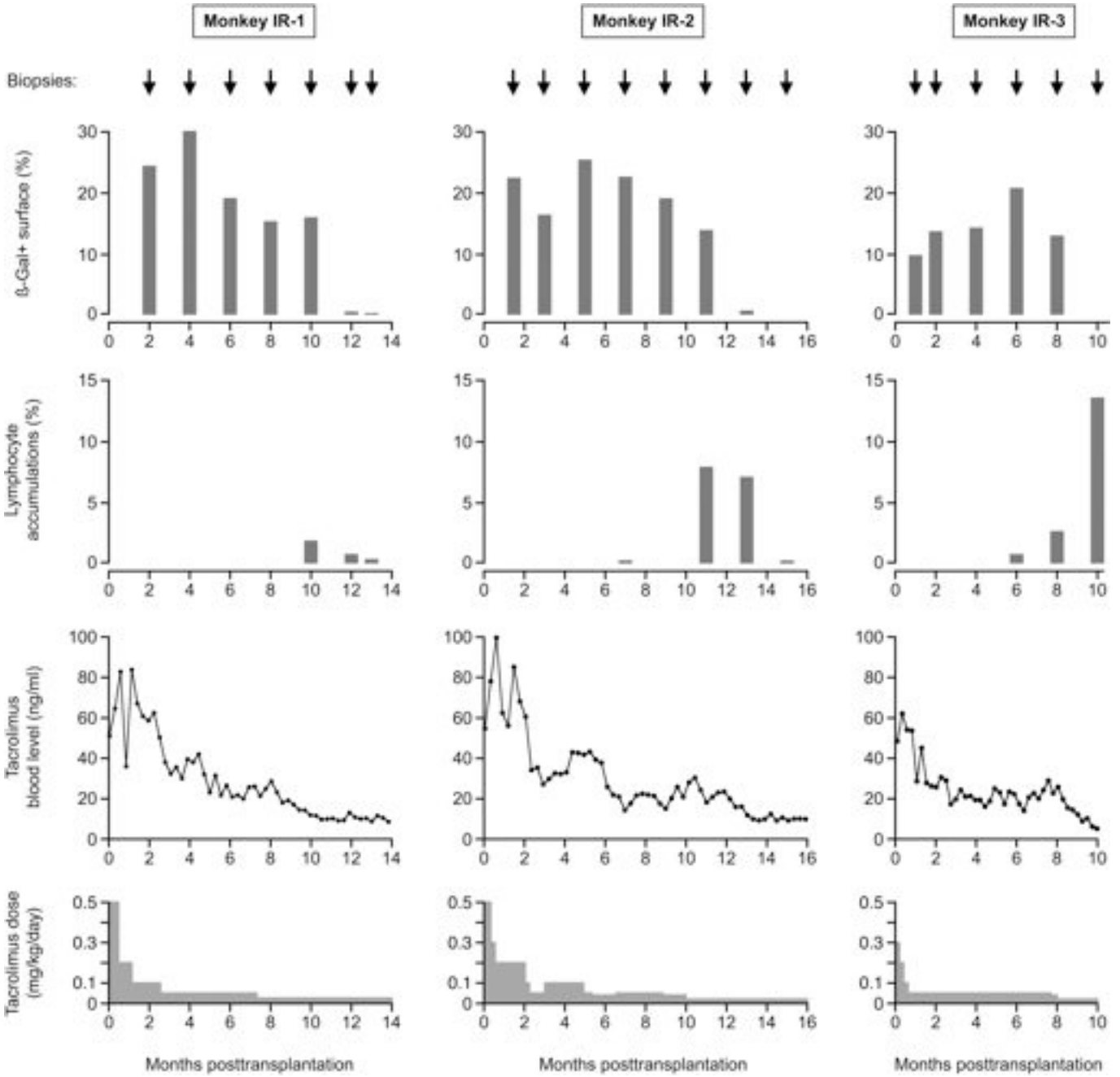

FIGURE 5. Graphical representation of the evolution of the graft and lymphocyte accumulations in 3 monkeys of the immunosuppression reduction (IR) group. The temporal correlation between graft loss and lymphocyte infiltration is evident and can be compared to tacrolimus blood levels. The bottom row graphs show the doses of tacrolimus administered to each monkey. Arrows indicate the biopsy time points. The y axes are at the same scale for each parameter.

were performed at 1 month after transplantation and then every 2 weeks until the graft was absent in at least 2 consecutive biopsies. In the LI group, they were performed 4, 12 (4 monkeys), and 20 weeks (3 monkeys) after transplantation. In the IR group, they were performed at 1 month after transplantation, and then every 1 to 2 months until graft rejection was observed. Biopsies were mounted in embedding medium and snap frozen in liquid N_2. Serial sections of 10 to 15 Km were made in a cryostat.

Histology

Sections were stained routinely with hematoxylin and eosin (H&E). For histochemical detection of A-Gal, the sections

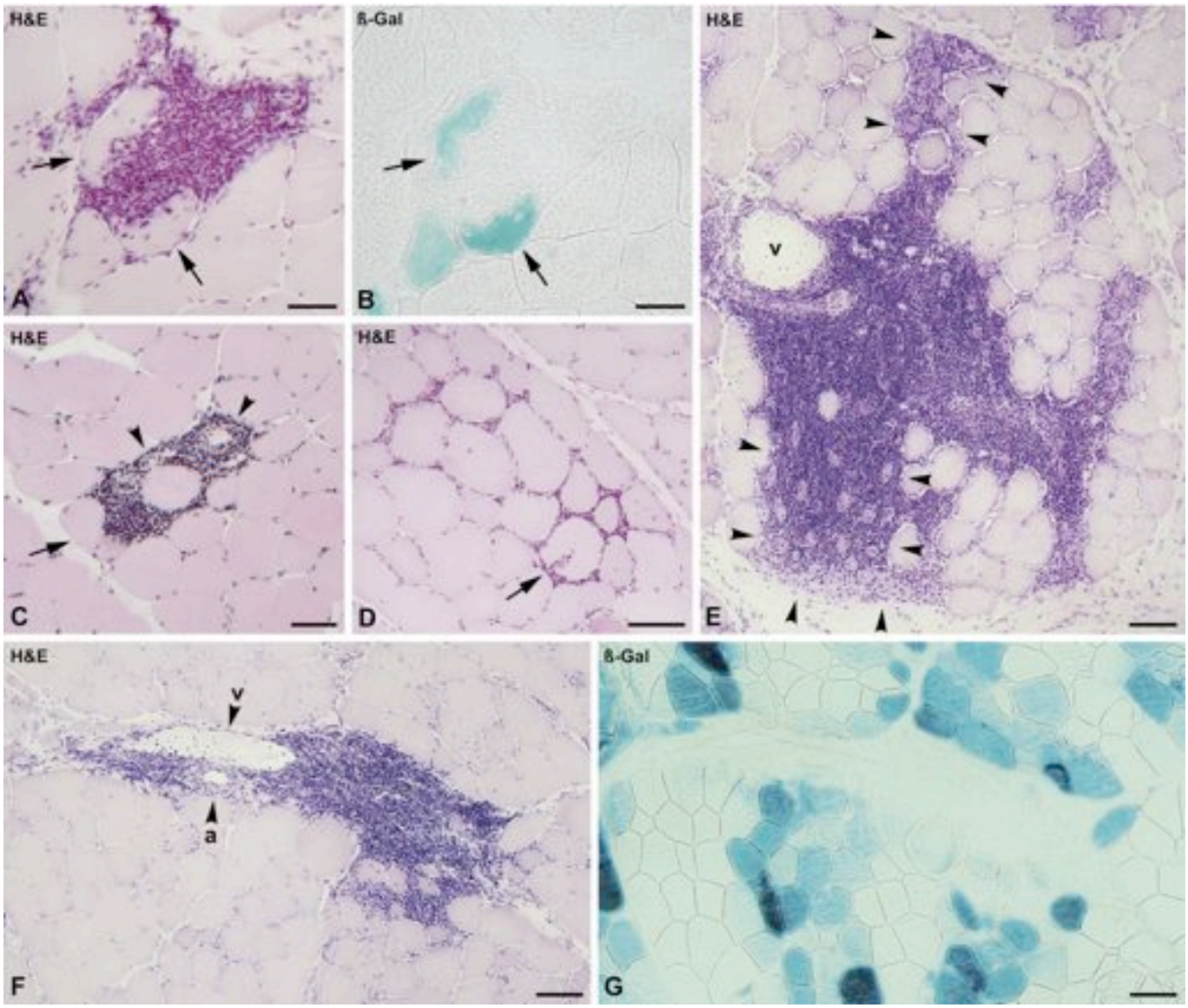

FIGURE 6. Appearances of focal lymphocyte accumulations. (AYC) Typical examples of lymphocyte invasion of nonnecrotic myofibers (arrows). (A) From the low-immunosuppression (LI) group (monkey LI-4) at 4 weeks after transplantation; in a serial section, invaded myofibers are A-galactosidase (A-Gal) positive (B, arrows). (C) From monkey LI-1 at 20 weeks after transplantation (arrowheads indicate small vessels). (D) Biopsy from immunosuppression withdrawal (IW) monkey-1 at 10 weeks after tacrolimus withdrawal shows very small endomysial lymphocyte accumulation with focal invasion of a nonnecrotic myofiber (arrow). (E) A large accumulation of lymphocytes associated with a venule (v), corresponding to the peak of infiltration in monkey IW-3 at 6 weeks after tacrolimus withdrawal. Regenerating myofibers are indicated between arrowheads; those in the lower portion of the panel are surrounded by lymphocytes. (F) Focal perivascular accumulation of lymphocytes around vessels in the perimysium (left side of field) (v, venule; a, arteriole) infiltrate the muscle bundles (right side); biopsy is from monkey IW-2 at 6 weeks after tacrolimus withdrawal, before the peak of infiltration. (G) Serial section of F showing that myofibers in the region are A-Gal positive. Scale bars = (AYC) 50 Km; (DYG) 100 Km.

were fixed 3 minutes in 0.25% glutaraldehyde, rinsed with phosphate-buffered saline (PBS), incubated 24 hours at room temperature in a solution of 0.4 mg/mL X-gal (5-bromo-4-chloro-3-indolyl-A-D-galactopyranoside) (Boehringer Mannheim, Vienna, Austria) containing 1 mmol/L $MgCl_2$, 3 mmol/L $Ke_3F(CN)_6l3$ mmol/L $Ke_4F(CN)_6l3H_2O$ in PBS, and mounted in 1:1 glycerin jelly.

For immunohistochemistry, the following mouse anti-human monoclonal antibodies (mAbs) were used: anti-CD8 mAb (BD Biosciences, Mississauga, Ontario, Canada), anti-CD4 mAb (BD Biosciences), anti-human CD163 mAb for macrophages (BD Biosciences), and a mouse anti-human eosinophils mAb (BD Biosciences).

For immunohistology, nonspecific binding was blocked by a 30-minute incubation with 10% fetal bovine serum in PBS. Thereafter, sections were incubated 1 hour with the primary antibody at concentrations recommended by the manufacturers, followed by a 30-minute incubation with biotinylated anti-mouse antibody (1:150; Dako, Glostrup, Denmark) and a 30-minute incubation with streptavidin-Cy3 (1:700; Sigma). Antibodies and streptavidin were diluted in PBS, pH 7.4, with 1% fetal bovine serum. Incubations were at room temperature. Reactivities of the mAbs to cynomolgus monkey cells were confirmed before the study.

Microscopy

The muscle cross sections were analyzed using an Axiophot microscope with epifluorescent and bright field optics (Zeiss, Oberkochen, Germany), and pictures were obtained with a digital camera A650 IS (Canon, Tokyo, Japan). To quantify the graft, we estimated the percentage of the sectional area of the muscle fascicles that was A-Gal positive. We also quantified the percentage of the sectional area of the grafted muscle occupied by lymphocyte accumulations. These areas were measured using a computer image analyzer (NIH Image 1.61, Bethesda, MD).

PCR Detection of Y Chromosome

Total DNA was extracted from cryostat sections of muscle biopsies performed in the 3 female macaques in the IW group that were grafted with male myoblasts (A-Gal negative). We also extracted the total DNA from cryostat sections of a biopsy performed on a male macaque as a positive control. Polymerase chain reaction was done with the oligonucleotide primers (32), namely, J130, 5¶-CGTGTCTT TCCTCATGGCTTC-3¶ (forward) and macaque CDY-2r, 5¶-CTTTACCATGGATTCGACCC-3¶ (reverse), engineered to amplify a 1610-bp region of the cynomolgus Y chromosome. Polymerase chain reaction conditions were as follows: 1 cycle

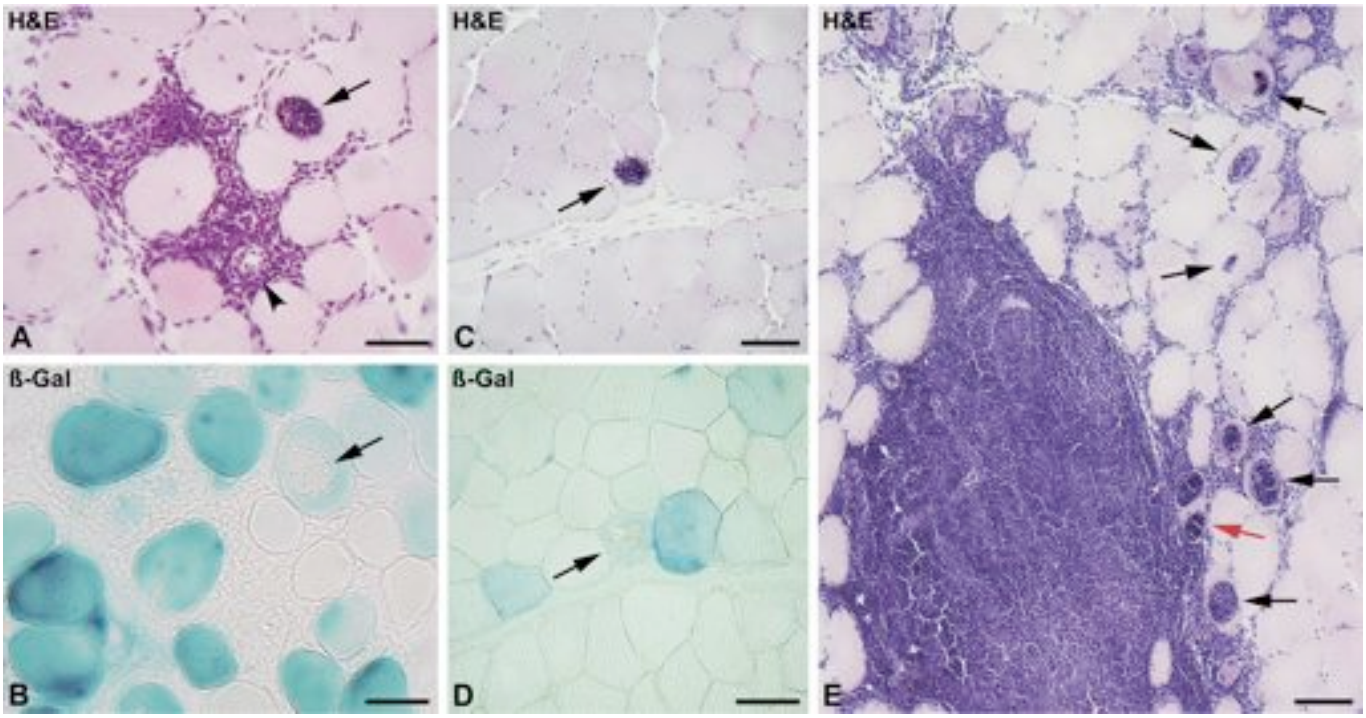

FIGURE 7. Tunneling pattern of myofiber invasion by lymphocyte infiltrates. (A) Biopsy from a low-immunosuppression (LI) monkey LI-1 at 1 month after transplantation shows a myofiber with a typical central lymphocyte accumulation (arrow) near a focal endomysial lymphocyte accumulation. This infiltration is also perivascular (vessel indicated by arrowhead). (B) Adjacent serial section stained for A-galactosidase (A-Gal) shows that the invaded myofiber is A-Gal positive (arrow). (C) The less frequent pattern of a myofiber with tunneling invasion apparently isolated if the lymphocyte accumulation is out of the cross section (arrow) (monkey IR-1, 12 months after transplantation). (D) The adjacent serial section stained for A-Gal shows that the invaded myofiber is A-GalYpositive (arrow). (E) In some cases of intense lymphocyte infiltration, several myofibers show a tunneling pattern of invasion of different intensity (arrows). An exceptional example of a myofiber with 2 lymphocyte ''tunnels'' is indicated with a red arrow. This biopsy is from monkey IR-3 10 months after transplantation; there were no A-GalYpositive myofibers remaining at that time. Scale bars = (A, B) 50 Km; (CYE) 100 Km.

at 95-C for 10 minutes; 30 cycles at 95-C for 1 minute, 66-C for 1 minute, and at 72-C for 1 minute; and 1 cycle at 72-C for 10 minutes. The PCR products were loaded on 1% agarose gel, and the DNA stained with ethidium bromide was scanned with an AlphaImager digital imaging system, avoiding saturation. RAG gene DNA was detected to control the quality of the extracted DNA. Water (instead of DNA) was used as a negative control.

RESULTS

Graft Rejection in the IW Group

In monkeys that received transplantation of A-GalY labeled myoblasts, the graft was monitored by the detection of A-GalYpositive myofibers (Figs. 1AYD). Figure 2 shows the evolution of the graft plotting the surface of the muscle sections that was A-Gal positive. AT 4 weeks after transplantation (the time of the tacrolimus withdrawal), A-GalYpositive myofibers covered 10.7%, 27.8%, and 35% of the muscle sections (Fig. 2). With variations, quite similar amounts of A-GalY positive myofibers were observed up to 4 to 6 weeks after the tacrolimus withdrawal (Fig. 2). Thereafter, A-GalYpositive myofibers disappeared either abruptly or after a drastic decrease in density and staining (Figs. 1C, D, and 2).

In female monkeys that received transplantation of male nonYA-GalYlabeled myoblasts, a PCR product corresponding to the Y chromosome was observed up to 6, 8, or 10 weeks after tacrolimus withdrawal (Fig. 3). The last band detected was generally weaker than that in the preceding biopsy and the Y-chromosome was not detected in subsequent biopsies.

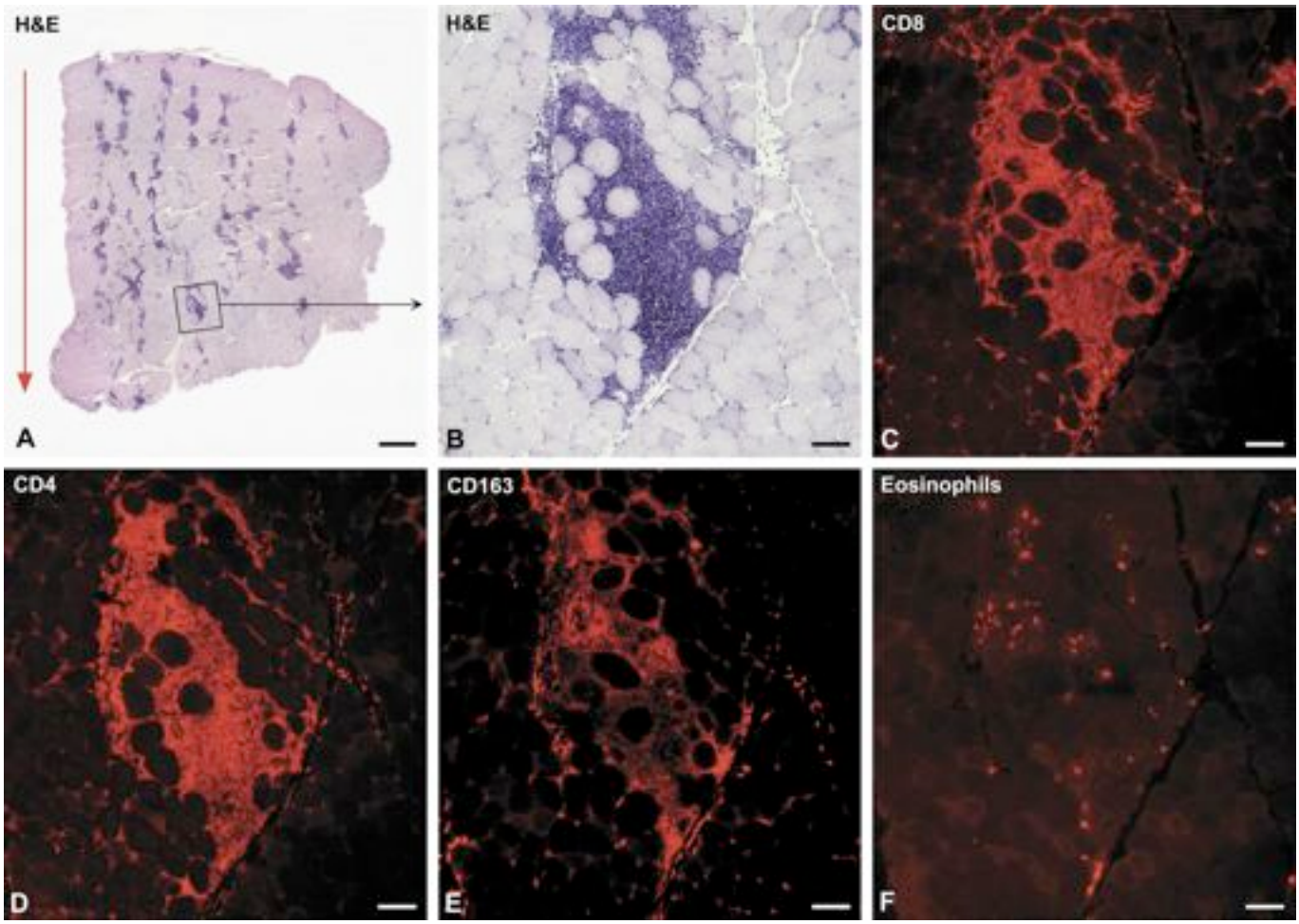

FIGURE 8. Localization of immune cells in serial sections of a muscle biopsy performed in a grafted site in a monkey allotransplanted with A-galactosidase (A-Gal)Ynegative myoblasts in the immunosuppression withdrawal (IW) group at the peak of lymphocyte infiltration. (A, B) The entire cross section is shown stained with hematoxylin and eosin (A); the muscle surface is at the top where the epimysium can be seen. There are several foci of lymphocytic infiltration that are roughly arranged in parallel ''stripes'' from the surface to the deep region of the biopsy and are reminiscent of the trajectory of the cell injections (red arrow). This pattern is similar to that observed when allogeneic myofibers are identified (45) and is further confirmation that lymphocyte accumulations are related to the graft. The square in A is enlarged in B to show myofibers partially or completely surrounded by lymphocytes. (CYF) Serial cross sections of the region in B show by fluorescent staining that this focal accumulation is mainly composed of CD8-positive (C) and CD4-positive (D) cells. Macrophages (E, CD163-positive) associated with the lymphocyte cluster are mostly around the myofibers. Some eosinophils are observed (F). Scale bars = (A) 1 mm; (BYF) 100 Km.

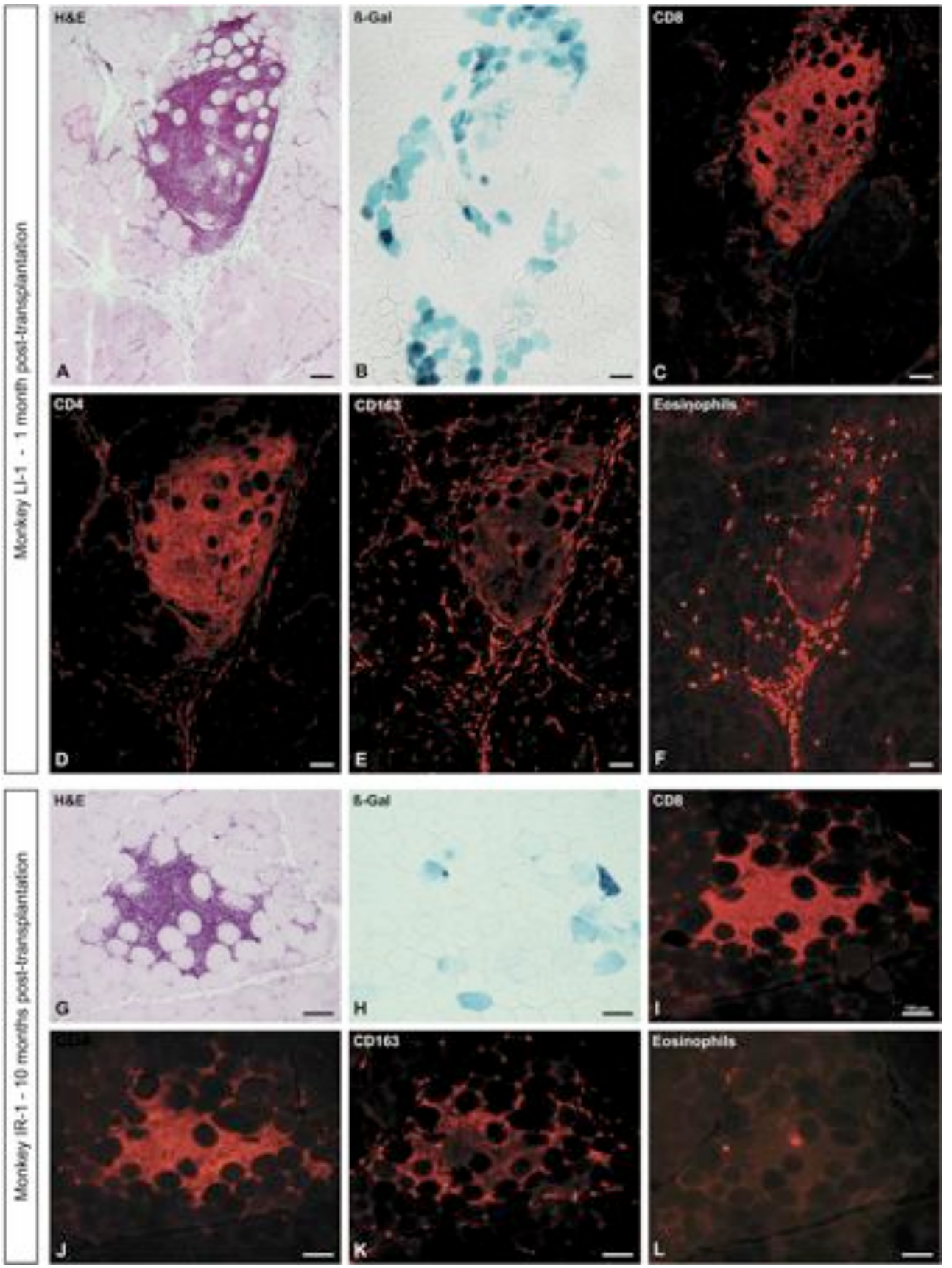

Main Histopathologic Changes Associated With Graft Loss in the IW Group

In all cases, the major histopathologic change in H&E-stained sections was focal infiltration of the muscle by dense clumps of mononuclear cells (Figs. 1EYJ and 3, bottom). Most cells in these accumulations had hyperchromatic round nuclei and thin cytoplasm characteristic of lymphocytes (Fig. 1J).

The area occupied by focal lymphocyte accumulations in the muscle sections was quantified to plot their evolution (Figs. 2 and 3). In each monkey, lymphocyte infiltration was very intense in 1 of the biopsies (Figs. 1G, I, and 3, bottom), producing a peak in the graphs (Figs. 2 and 3). In different animals, this peak was observed at 6, 8, 10, or 14 weeks after the tacrolimus withdrawal. It appeared suddenly or was preceded by a mild-to-moderate infiltration 2 to 6 weeks earlier (Figs. 1F, 2, and 3). It was followed by a mild or moderate infiltration that progressively decreased (Figs. 1H, 2, and 3). The intensity of the peak of infiltration was quite similar among the 6 monkeys: from approximately 14% to 25.5% of the muscle cross section was covered by lymphocyte accumulations (mean = 17.5% T 4.2% [SD]).

In monkeys that received transplantation of A-GalYlabeled myoblasts, the peak of lymphocyte infiltration correlated with the abrupt decrease or with the disappearance of A-GalYpositive myofibers (Figs. 1AYH and 2). In monkeys that received allotransplantations of myoblasts nonYA-Gal labeled, the peak of infiltration correlated with a decrease in the intensity of the band corresponding to the Y chromosome or its disappearance (Fig. 3). In conclusion, the focal dense lymphocyte accumulations correlated with the graft loss in the 6 monkeys.

Association of Rejection With Tacrolimus Blood Levels in the IW Group

Tacrolimus blood levels gradually decreased after tacrolimus withdrawal, until the complete disappearance 7 to 9 weeks later (Figs. 2 and 3). Graft loss and acute lymphocyte infiltration occurred when the tacrolimus blood levels were below 10 Kg/L (Figs. 2 and 3).

Comparison of A-GalYExpressing Versus A-GalYNegative Myofibers

The histopathology and immune cells involved were similar for the transplantation of A-GalYlabeled and non A-GalYlabeled cells. Thus, the expression of A-Gal had no effect on the histologic pattern of rejection. In consequence, the experimental LI and IR groups only had transplantation of A-GalYlabeled cells. This allowed histologic monitoring of the graft and correlation between A-GalYpositive myofibers and immune cells.

Graft Rejection in the LI Group

Tacrolimus blood levels ranged between 38 and 18 Kg/L during follow-up (Fig. 4). Biopsies performed 4 weeks after transplantation showed abundant A-GalYpositive myofibers, which covered 16.6% to 53.1% of the muscle sections (Fig. 4). In biopsies performed 12 and 20 weeks after transplantation, the amount of A-GalYpositive myofibers decreased significantly and finally disappeared in 3 monkeys (Fig. 4). Therefore, the graft was lost during the follow-up.

Biopsies performed at 4 weeks after transplantation showed inflammation in the regions containing A-GalY positive myofibers (Fig. 4). The prominent feature of this infiltration in the H&E-stained sections was the presence of focal lymphocyte accumulations, similar to those in the IW group. The lymphocyte infiltration was not as intense as at the peak of infiltration in the IW group, but they were similar to the levels of infiltration before or after this peak.

Graft Rejection in the IR Group

Tacrolimus blood levels during the first month after transplantation were at an average of 75.9, 70.5, and 48.6 Kg/L. They then gradually decreased as the dose of tacrolimus was reduced, reaching values around 10 Kg/L after 41, 47, and 40 weeks, respectively, after transplantation (Fig. 5). A-GalY positive myofibers were observed for several months after transplantation (Fig. 5). However, tacrolimus blood levels could not be maintained between 20 and 10 Kg/L for several weeks without causing graft loss (Fig. 5).

Main Histopathologic Changes Associated to Graft Loss in the IR Group

The main histopathologic change in H&E-stained sections during the follow-up of 43, 55, and 65 weeks was muscle tissue infiltration by focal lymphocyte accumulations that correlated with loss of A-GalYpositive myofibers in the 3 monkeys (Fig. 5). The maximum intensity of infiltration in the biopsies was variable. Before this lymphocyte infiltration, the histologic finding from the muscle biopsy was normal, except for some central nuclei as a sign of previous regeneration (resulting from the myofiber damage produced during transplantation).

Histologic Characteristics of the Acute Rejection

The histologic characteristics of the immune cell infiltration in all the monkeys were similar, with the only difference

FIGURE 9. Localization of immune effector cells in serial cross sections of 2 muscle biopsies at grafted sites in monkeys of the low-immunosuppression (LI) (AYF) and immunosuppression reduction (IR) (GYL) groups illustrate the homogeneity of the immune cell participation, independent of the expression of A-galactosidase (A-Gal) (compare with Fig. 8) and the time of acute rejection. In both cases there are focal accumulations of lymphocytes (A, G) associated with A-GalYpositive myofibers (B, H). Fluorescent stains show that these accumulations are mainly composed of CD8-positive (C, I) and CD4-positive (D, J) lymphocytes. CD8-positive lymphocytes are scarce outside the foci, but CD4-positive lymphocytes are also seen diffusely in the endomysium and perimysium. Macrophages (CD163-positive) are present in lower amounts than lymphocytes in the focal accumulations but are abundant diffusely through the endomysium and perimysium (E, K). Macrophages associated with lymphocyte clusters are also mostly around myofibers. Several eosinophils are observed in F (mainly in the perimysium but also in the endomysium and between lymphocytes), but few are seen in L. Scale bars = 100 Km.

being the intensity of infiltration over time. Given this homogeneity, the three experimental groups (IW, LI and IR) are considered here together.

The focal lymphocyte accumulations predominated in the endomysium, surrounding totally or partially some myofibers (Figs. 1J, 4B, 6AYE, 7A, 8B, and 9A, G). Some lymphocyte accumulations were present in the perimysium, although mostly in continuity with endomysial infiltration (Figs. 4B and 6F). They were frequently part of perivascular focal cellular exudates around small vessels in the perimysium, showing the migration of lymphocytes from venules toward myofibers (Figs. 6F, G). Focal perivascular lymphocyte exudates were also observed around smaller vessels in the muscle bundles, showing also migration from the vessels to the myofibers (Figs. 6C and 7A).

The partial invasion of nonnecrotic myofibers by surrounding mononuclear cells was frequent (Figs. 1J and 6AYD). The degree of invasion was variable and was either focal or around the myofiber perimeter. In some cases, a ''tunneling'' pattern of invasion was observed (Fig. 7). Myofibers with tunneling pattern of lymphocyte invasion were frequently near endomysial lymphocyte accumulations (Figs. 7A, B) but were isolated in some cases (Figs. 7C, D), indicating that there was lymphocyte penetration from regions outside the planes of section. Most myofibers located in or around the focal lymphocyte accumulations were not necrotic. Lymphocyte invasion of nonnecrotic myofibers was frequent in cases of moderate infiltration (G5% of the muscle cross section).

In biopsies with intense lymphocyte infiltration (i.e. the peak of infiltration in the IW group and at 10 months in monkey IR-3), myofibers showed more severe alterations than in the cases of moderate infiltration (Figs. 6E and 7E). Some necrotic myofibers, often undergoing phagocytosis, were observed. Myotubes or small myofibers undergoing regeneration were also observed, characterized by central enlarged nuclei and sarcoplasmic basophilia (Fig. 6E). Myofiber regeneration results from recent myofiber necrosis, which may indicate that there was myofiber necrosis due to the intense and rapid attack of lymphocytes. Myofibers with tunneling invasion by lymphocyte were more abundant (Fig. 7E). Whorled myofibers and myofibers with multiple internal splitting were also observed.

Effector Cells in the Inflammatory Infiltrates

Similar inflammatory cell phenotypes were observed in the 3 treatment groups. CD8-positive cells were homogeneously and densely distributed throughout the lymphocyte accumulations (Figs. 8C and 9C, I). They were so closely packed that it was difficult to distinguish individual cells at low magnification. Few CD8-positive cells were observed outside the lymphocyte accumulations. CD8-positive cells were scarce in muscle biopsies that preceded the infiltration by focal dense lymphocyte accumulations (IW and IR groups); in those cases, they were mostly seen as isolated cells in the endomysium and perimysium, sometimes in perivascular locations.

CD4-positive cells were also homogeneously and densely distributed (Figs. 8D and 9D, J). These cells were also so closely packed that individual cells were difficult to distinguish at low magnification. Some CD4-positive cells were observed outside the lymphocyte accumulations, dispersed in the endomysium, perimysium, and epimysium. Dispersed CD4-positive cells were also observed in the muscle biopsies that preceded the infiltration by the focal dense lymphocyte accumulations (IW and IR groups).

CD163-positive cells (macrophages) were observed in the focal lymphocyte accumulations and in forming a diffuse infiltration in the endomysium, perimysium, and epimysium (Figs. 8E and 9E, K). In the focal lymphocyte accumulations, they were less abundant than CD4-positive and CD8-positive cells and were found mainly in the periphery of the accumulations, around some myofibers and invading necrotic myofibers. CD163-positive cells were the most abundant immune cells in the diffuse infiltration of immune cells in the endomysium, perimysium, and epimysium and were observed in the muscle biopsies preceding the infiltration by the focal dense lymphocyte accumulations in the IW and IR groups.

Eosinophils were present as isolated cells in perivascular, perimysial, and endomysial areas and, although not always, as part of the focal lymphocyte accumulations. They were observed at the peak of lymphocyte infiltration in the IW group (Fig. 8F), mostly at 4 weeks after transplantation in the LI group (Fig. 9F) and at the peak of lymphocyte infiltration in the IR group (Fig. 9L).

DISCUSSION

Acute rejection of myofibers in macaques that received myoblast allotransplantation was observed in different experimental conditions. Transplantation of A-GalYpositive myoblasts allowed histologic monitoring of the grafts and topographical correlation with immune cells. Transplantation of nonYA-GalY labeled cells indicated that the results were not due to the expression of A-Gal. The IW group was designed to induce acute rejection of myofibers; the LI and IR groups showed that the histologic pattern of acute rejection was the same in conditions more similar to clinical scenarios in which a graft recipient receives continuous immunosuppression regardless of whether rejection occurs at the beginning (LI group) or several months (IR group) after transplantation.

Graft loss occurred with stereotypical histologic features in all monkeys when there were low levels of immunosuppression. The most conspicuous of these was the presence of focal, mostly endomysial lymphocyte accumulations that typically surrounded myofibers (partially or completely) and frequently invaded some of them. CD4-positive and CD8-positive cells were most abundant with a lesser component of macrophages. Eosinophils were observed in almost all cases but in smaller amounts than the other cells and not always in the lymphocyte accumulations. The only differences among biopsies were the amounts and sizes of the lymphocyte accumulations. In addition, more intense lymphocyte infiltrations had more associated myofiber reactions, such as necrotic, regenerating, and whorled myofibers. The more intense lymphocyte infiltration appeared to be associated with rapid rejection, when there were too low blood levels of tacrolimus. Perhaps this difference in intensity might be used in the future for grading acute rejection of myofibers, as is currently done in organ transplantation (33, 34).

Although the aim of this study was to provide essential clues to the histologic diagnosis of myofiber rejection and not to perform an analysis of the mechanisms of rejection, some considerations are pertinent. There are essentially 4 pathways of allograft rejection: direct cytotoxicity of CD8-positive lymphocytes, delayed-type hypersensitivity of macrophages activated by T_H1 CD4-positive lymphocytes, FasL-dependent cytotoxicity of CD4-positive lymphocytes, and eosinophil-mediated damage elicited by T_H2 CD4-positive cells (35). These effector cell populations were detected during rejection in the present study, but because there were few eosinophils, especially in comparison to the other cells, we exclude a priori a key role for them. Indeed, the pivotal role in myofiber rejection seems to be played by CD8-positive and CD4-positive lymphocytes. The presence of diffuse infiltration of macrophages, even in optimal immunosuppression without graft rejection, seems to be a consequence of the tissue damage produced by the several injections used for transplantation.

The present results should be compared to previous clinical observations regarding immune reactions in skeletal muscle. Studies of acute rejection in vascularized skeletal-muscle allotransplantation are scarce, and have few histological details (36). Moreover, the histologic manifestations in vascularized grafts are complicated by the importance of endothelial rejection (37), which is absent in myoblast transplantation because the vessels are those of the recipient. The most detailed analyses of immune reactions in human skeletal muscle have been performed in autoimmune myopathies. In fact, there are interesting similarities between our observations and the histopathology of polymyositis and sporadic inclusion body myositis (38). These conditions are considered to be autoimmune myopathies in which the pathogenesis is MHC-restricted cytotoxicity of CD8-positive T lymphocytes against myofibers (39). As in the present study, the predominant histologic feature in both autoimmune myopathies is the presence of focal accumulations of T lymphocytes and macrophages, partially or completely surrounding some myofibers (40, 41). Also similar is the presence of lymphocytes invading nonnecrotic myofibers (12, 40, 41), sometimes also producing ''tunneling'' invasion (42). This may indicate that there is homogeneity in the pattern of the immune attack against myofibers, independently of whether this is in the context of acute rejection or in the context of autoimmune myopathy. This could also indicate that in our case the most important mechanism of rejection is similar to that of these autoimmune myopathies, that is, a direct MHC-restricted cytotoxicity of CD8-positive T lymphocytes, causing myofiber necrosis through a granzyme-mediated pathway (43, 44). Further studies are needed to confirm that mechanism.

The present results can also be compared to the few studies in which myofiber rejection was observed after withdrawal of immunosuppression in mice (15, 17). Using toluidine blue staining, mouse studies reported massive infiltration of myoblast-grafted muscles by ''darkly stained mononuclear cells'' with characteristics of lymphocytes and macrophages, associated with myofiber regeneration and necrosis. This occurred at 1 month after immunosuppression withdrawal and 2 months after transplantation, comparable to our results in the IW group. However, massive infiltration with mononuclear cells was still observed 3 to 6 months later, together with muscle fibrosis, whereas in macaques, the lymphocyte infiltration resolved faster and there was no fibrosis. In contrast, also with the present study, transient immunosuppression (only for 2 weeks) allowed immune tolerance to myoblast transplantation in mice (13), whereas we observed rapid rejection in monkeys. These disparities emphasize the transplantation immunology differences between mice and primates.

Finally, it is particularly important to compare the inflammatory reactions observed in this study with those observed in clinical trials of myogenic cell transplantation. As mentioned above, the only histologic analysis of the immune cell reactions in this context is our last clinical trial of myoblast allotransplantation (5). In that study, muscle biopsies performed in myoblast-grafted sites in some patients showed immune infiltrates with the morphologic patterns described here, that is, there were focal lymphocyte accumulations surrounding partially or completely myofibers expressing donor-derived proteins. Moreover, in some cases, we observed lymphocyte invasion of nonnecrotic myofibers expressing donor-derived proteins, both as a peripheral focal invasion and as a tunneling invasion. As in the present study, CD8-positive and CD4-positive lymphocytes were the main cells in the focal lymphocyte accumulations, with a component of macrophages. As in monkeys, few CD8-positive cells were observed outside the focal accumulations, some CD4-positive cells were observed isolated in the endomysium, perimysium, and epimysium, and macrophages were abundant throughout the muscle tissue and were present both in the focal lymphocyte accumulations and as a diffuse infiltration in the endomysium, perimysium, and epimysium. These similarities may further validate the relevance of our present observations to the clinical setting.

In conclusion, the histologic feature that enables diagnosing acute rejection of myofibers expressing allogeneic proteins is the presence of focal dense endomysial accumulations of CD8-positive and CD4-positive lymphocytes, with a component of macrophages, partially or completely surrounding the myofibers. The presence of lymphocyte invasion of myofibers further supports the diagnosis, but it should not be a requirement because it is not evident in all the lymphocyte accumulations.

ACKNOWLEDGMENTS

The author wishes to express his gratitude to Mrs Marlyne Goulet and Mr Martin Paradis for their excellent technical work in cell culture, immunohistochemistry, PCR, and follow-up of immunosuppression in monkeys and to Dr Jacques P. Tremblay for providing laboratory facilities.

REFERENCES

1. Skuk D. Myoblast transplantation for inherited myopathies: A clinical approach. Expert Opin Biol Ther 2004;4:1871Y85
2. Neil DA, Hubscher SG. Current views on rejection pathology in liver transplantation. Transpl Int 2010;23:971Y83
3. Patel JK, Kittleson M, Kobashigawa JA. Cardiac allograft rejection. Surgeon 2011;9:160Y67

4. Henderson LK, Nankivell BJ, Chapman JR. Surveillance protocol kidney transplant biopsies: Their evolving role in clinical practice. Am J Transplant 2011;11:1570Y75
5. Skuk D, Goulet M, Roy B, et al. Dystrophin expression in muscles of Duchenne muscular dystrophy patients after high-density injections of normal myogenic cells. J Neuropathol Exp Neurol 2006;65:371Y86
6. Skuk D, Goulet M, Roy B, et al. First test of a "high-density injection" protocol for myogenic cell transplantation throughout large volumes of muscles in a Duchenne muscular dystrophy patient: Eighteen months follow-up. Neuromuscul Disord 2007;17:38Y46
7. Kinoshita I, Vilquin JT, Guerette B, et al. Immunosuppression with FK 506 insures good success of myoblast transplantation in MDX mice. Transplant Proc 1994;26:3518
8. Kinoshita I, Vilquin JT, Guerette B, et al. Very efficient myoblast allotransplantation in mice under FK506 immunosuppression. Muscle Nerve 1994;17:1407Y15
9. Kinoshita I, Roy R, Dugre FJ, et al. Myoblast transplantation in monkeys: Control of immune response by FK506. J Neuropathol Exp Neurol 1996; 55:687Y97
10. Skuk D, Goulet M, Roy B, et al. Myoblast transplantation in whole muscle of nonhuman primates. J Neuropathol Exp Neurol 2000;59:197Y206
11. McDouall RM, Dunn MJ, Dubowitz V. Nature of the mononuclear infiltrate and the mechanism of muscle damage in juvenile dermatomyositis and Duchenne muscular dystrophy. J Neurol Sci 1990;99:199Y217
12. Arahata K, Engel AG. Monoclonal antibody analysis of mononuclear cells in myopathies. IV: Cell-mediated cytotoxicity and muscle fiber necrosis. Ann Neurol 1988;23:168Y73
13. Pavlath GK, Rando TA, Blau HM. Transient immunosuppressive treatment leads to long-term retention of allogeneic myoblasts in hybrid myofibers. J Cell Biol 1994;127:1923Y32
14. Guerette B, Asselin I, Vilquin JT, et al. Lymphocyte infiltration following allo- and xenomyoblast transplantation in mdx mice. Muscle Nerve 1995; 18:39Y51
15. Irintchev A, Zweyer M, Wernig A. Cellular and molecular reactions in mouse muscles after myoblast implantation. J Neurocytol 1995;24:319Y31
16. Wernig A, Irintchev A. "Bystander" damage of host muscle caused by implantation of MHC- compatible myogenic cells. J Neurol Sci 1995; 130:190Y96
17. Wernig A, Irintchev A, Lange G. Functional effects of myoblast implantation into histoincompatible mice with or without immunosuppression. J Physiol (Lond) 1995;484:493Y504
18. Skuk D, Caron NJ, Goulet M, et al. Dynamics of the early immune cellular reactions after myogenic-cell transplantation. Cell Transplant 2002; 11:671Y81
19. Mestas J, Hughes CC. Of mice and not men: Differences between mouse and human immunology. J Immunol 2004;172:2731Y38
20. Rose SM, Blustein N, Rotrosen D. Recommendations of the expert panel on ethical issues in clinical trials of transplant tolerance. National Institute of Allergy and Infectious Diseases of the National Institutes of Health. Transplantation 1998;66:1123Y25
21. Kirk AD. Transplantation tolerance: A look at the nonhuman primate literature in the light of modern tolerance theories. Crit Rev Immunol 1999;19:349Y88
22. Kirk AD. Crossing the bridge: Large animal models in translational transplantation research. Immunol Rev 2003;196:176Y96
23. Slierendregt BL, van Noort JT, Bakas RM, et al. Evolutionary stability of transspecies major histocompatibility complex class II DRB lineages in humans and rhesus monkeys. Hum Immunol 1992;35:29Y39
24. Geluk A, Elferink DG, Slierendregt BL, et al. Evolutionary conservation of major histocompatibility complex-DR/peptide/T cell interactions in primates. J Exp Med 1993;177:979Y87
25. Jaeger EE, Bontrop RE, Lanchbury JS. Structure, diversity, and evolution of the T-cell receptor VB gene repertoire in primates. Immunogenetics 1994;40:184Y91
26. Levinson G, Hughes AL, Letvin NL. Sequence and diversity of rhesus monkey T-cell receptor beta chain genes. Immunogenetics 1992;35:75Y88
27. Cendales LC, Xu H, Bacher J, et al. Composite tissue allotransplantation: Development of a preclinical model in nonhuman primates. Transplantation 2005;80:1447Y54
28. Ham RG, St. Clair JA, Webster C, et al. Improved media for normal human muscle satellite cells: Serum-free clonal growth and enhanced growth with low serum. In Vitro Cell Dev Biol 1988;24:833Y44
29. Skuk D, Goulet M, Paradis M, et al. Myoblast transplantation: Techniques in nonhuman primates as a bridge to clinical trials. In: Soto-Gutierrez A, Navarro-Alvarez N, Fox IJ, eds. Methods in Bioengineering: Cell Transplantation. Boston, MA: Artech House, 2011;219Y36
30. Skuk D, Goulet M, Tremblay JP. Use of repeating dispensers to increase the efficiency of the intramuscular myogenic cell injection procedure. Cell Transplant 2006;15:659Y63
31. Richard PL, Gosselin C, Laliberte T, et al. A first semimanual device for clinical intramuscular repetitive cell injections. Cell Transplant 2010;19: 67Y78
32. Kostova E, Rottger S, Schempp W, et al. Identification and characterization of the cynomolgus monkey chromodomain gene cynCDY, an orthologue of the human CDY gene family. Mol Hum Reprod 2002;8: 702Y9
33. Kozakowski N, Regele H. Biopsy diagnostics in renal allograft rejection: From histomorphology to biological function. Transpl Int 2009; 22:945Y53
34. Tan CD, Baldwin WM 3rd, Rodriguez ER. Update on cardiac transplantation pathology. Arch Pathol Lab Med 2007;131:1169Y91
35. Goldman M, Le Moine A, Braun M, et al. A role for eosinophils in transplant rejection. Trends Immunol 2001;22:247Y51
36. Jones TR, Humphrey PA, Brennan DC. Transplantation of vascularized allogeneic skeletal muscle for scalp reconstruction in a renal transplant patient. Transplantation 1998;65:1605Y10
37. Glotz D, Lucchiari N, Pegaz-Fiornet B, et al. Endothelial cells as targets of allograft rejection. Transplantation 2006;82:S19YS21
38. Dalakas MC. Muscle biopsy findings in inflammatory myopathies. Rheum Dis Clin North Am 2002;28:779Y98
39. Hohlfeld R, Engel AG, Goebels N, et al. Cellular immune mechanisms in inflammatory myopathies. Curr Opin Rheumatol 1997;9:520Y26
40. Arahata K, Engel AG. Monoclonal antibody analysis of mononuclear cells in myopathies. I: Quantitation of subsets according to diagnosis and sites of accumulation and demonstration and counts of muscle fibers invaded by T cells. Ann Neurol 1984;16:193Y208
41. Engel AG, Arahata K. Mononuclear cells in myopathies: Quantitation of functionally distinct subsets, recognition of antigen-specific cell-mediated cytotoxicity in some diseases, and implications for the pathogenesis of the different inflammatory myopathies. Hum Pathol 1986;17: 704Y21
42. Benveniste O, Dubourg O, Herson S. New classifications and pathophysiology of the inflammatory myopathies. Rev Med Interne 2007;28: 603Y12
43. Dalakas MC. Pathophysiology of inflammatory and autoimmune myopathies. Presse Med 2011;40:e237Y47
44. Dalakas MC. Review: An update on inflammatory and autoimmune myopathies. Neuropathol Appl Neurobiol 2011;37:226Y42
45. Skuk D, Goulet M, Roy B, et al. Efficacy of myoblast transplantation in nonhuman primates following simple intramuscular cell injections: Toward defining strategies applicable to humans. Exp Neurol 2002;175:112Y26